

# CLINOPYROXENE AND AMPHIBOLE ZONING PATTERNS IN TESCHENITE ROCKS FROM THE OUTER WESTERN POLISH CARPATIANS

R. WŁODYKA

*Department of Geochemistry and Petrology, Silesian University, Będzińska 60, 41-200 Sosnowiec, Poland*

**Abstract:** In the western part of the Outer Carpathians, between Bielsko-Biała and Cieszyn sills of teschenite and related rocks occur. Major element data support an *in situ* model for crystallisation of a primary teschenitic magma injected into wet flysch sediment at shallow depths. The compositional trends from diopside to hedenbergite and from kaersutite to ferro-kaersutite developed during fractional crystallisation of the melt.

**Key words:** teschenite rocks, diopside, hedenbergite, kaersutite, Poland

## INTRODUCTION

Mesozoic alkali basaltic intrusions of teschenitic affinity are widely distributed in the western part of the Outer Carpathians between Nowy Jičín (Czech Republic) and Cieszyn (Poland). Following Smulikowski (1980), they can be classified as picrites, teschenites and lamprophyres.

In a continuous vertical section through a teschenite sill, the following varieties of rocks can be distinguished: olivine teschenite, teschenite, syenoteschenite and syenite. The gradation from teschenite to syenoteschenite results from a progressive increase in the proportion of felsic mesostasis (sodic plagioclase, alkali feldspars and nepheline) and a decrease in the contents of olivine, clinopyroxene and amphibole. Syenite occurs only as small irregular bodies with sharp boundaries in the upper part of the sill or as veins cutting the upper chilled margins. In the syenite rocks alkali feldspars and nepheline constitute about 80 % of the rock.

The mafic minerals (pyroxene and amphibole) have not been affected by alteration. Thus, they should reliably record the complete magmatic crystallisation trends.

## RESULTS AND DISCUSSION

Representative major element analyses for all of the rocks from teschenite sill and for the felsic mesostasis are presented in Table 1 and Figure 1. The mineralogy and chemical composition of the syenite veins closely approximates to that of the felsic mesostasis in the teschenites and syenoteschenites. Major element data supports an *in-situ* model for crystallisation of the teschenite sill. It is probable that syenitic residual melt accumulated progressively during fractional

crystallisation of the mafic phases until it reached some critical volume whereupon it separated from a crystal mush to form the small irregular bodies. A part of the residua probably persisted to temperatures below the teschenite solidus and migrated towards the upper parts of intrusions forming cross-cutting veins.

*Clinopyroxenes* are among the most abundant minerals (up to 70 vol.%) in all rock types of the teschenite sill. They vary from microlites (<0.35 mm) in chilled margins to prismatic crystals about 1.5 mm across and 5mm long in teschenite and syenoteschenite. All pyroxenes exhibit typical sector zoning with pyramidal sectors enriched in Mg, Si, and depleted in Fe, Al and Ti, as compared to prismatic sectors. Core-to-rim variations within individual sectors principally involve substitution of iron for magnesium (Fig. 5). Concentric zoning is also common; the rims are enriched in Mn, Fe, Si and Na and depleted in Al, Mg, Ti and Ca.

The general compositional range of the pyroxene studied is shown on a pyroxene quadrilateral (Fig. 2) and in Table 2. Most of the clinopyroxene analyses plot above the Di-Hd join indicating the presence of non-quadrilateral components (high Ti and Al contents). The variations of Ti and Al in the prismatic and pyramidal sectors of the pyroxenes result in the scattering of projected points above the Di-Hd join. Generally, the clinopyroxene from teschenite and syenoteschenite plots in the field of diopside whereas the clinopyroxene from syenite plots in the field of hedenbergite.

Titanium and aluminium show the greatest variation in the pyroxenes studied. The contents of TiO<sub>2</sub> and Al<sub>2</sub>O<sub>3</sub> vary between 0.93–6.1% and 1.36–11.33% respectively. Figure 3a shows that, irrespective of teschenite rock type, the Al and Ti contents are closely related with Ti/Al about 0.25. Most of the pyroxenes studied plot in the “igneous clinopyroxene” field of the Al<sup>VI</sup> v. Al<sup>IV</sup> diagram of Aoki and Shiba (1973) as shown on Figure 3b. Titanium can enter the clinopyroxene structure together with two Al ions in the form of Ti-Tschermak’s molecule TiTs (Yagi and Onuma 1967). The lower Ti/Al found here compared with that in the TiTs molecule can be explained by the coupled substitution of CaTiAl<sub>2</sub>O<sub>6</sub> and CaAl<sub>2</sub>SiO<sub>6</sub> (CaTs) molecules in a ratio of about 1:1 (Gibb 1973). The solubility of Ti in diopside increases with increasing temperature whereas it decreases with increasing pressure (Yagi and Onuma 1967, Steep and Kunzmann 2001). Following Leung (1974), the sector-zoned titanaugites reflect rapid, disequilibrium crystallization at high temperature and relatively low pressure. All these observations point to the conclusion that the pyroxene investigated originated when primary teschenitic magma was injected into wet flysch sediments at shallow depths.

The variations in Ti, Al and Na contents during the course of crystallization are presented in Figure 4. The behaviour of Ti and Al is similar; both increase in pyroxenes from teschenites and

syenoteschenites and decrease in pyroxenes from syenite with decreasing *mg*-number. The Na<sub>2</sub>O content, which does not exceed 2%, increases continuously. The graph also shows the reaction between residual syenitic melt that migrated towards the upper level of the sill and early-formed pyroxene which display presence of green rims or mottled appearance. They plot within the areas indicated by the arrows on Figure 4. Although the late residual melts were highly alkaline, there is only a small increase in the aegirine component of the syenitic pyroxene. The compositional trend towards hedenbergite (Fig. 5) rather than aegirine is probably due to crystallization of the residual melts under conditions of lower oxygen fugacity and lower H<sub>2</sub>O content than those pertaining during crystallisation of the primary teschenitic magma (Gibb 1973).

*Amphiboles* vary in modal abundance from 2 vol.% (syenite) to 30 vol.% (mafic teschenite). They occur as microlites (<0.3 mm) in chilled margins or as prismatic crystals (up to 6mm long) in teschenite and syenoteschenite. In these rocks, there are numerous intergrowths of pyroxene and amphibole indicating their simultaneous crystallisation. There are also epitaxial growth relations indicative of amphibole nucleating after pyroxene. Amphibole is the major mafic phase in syenite where it typically forms needle-like crystals up to 10 mm in length. The compositional range of the amphibole studied is presented on Figure 2 and in Table 2. The amphiboles exhibit concentric zoning but not sector zoning. Core-to-rim variations mainly involve substitution of iron for magnesium. In the IMA amphibole classification, they correspond to kaersutite (core) and ferrokaersutite (rim). Green rims with hastingsite compositions originated during reaction with the late residual melts – as happened with pyroxene. Some kaersutite crystals are overgrown by later hedenbergite pyroxene.

## References

- AOKI K., SHIBA I., 1973: Pyroxene from lherzolite inclusions of Itinomegata, Japan. *Lithos* 6, 41-51.  
GIBB F. F.G. F., 1973: The zoned clinopyroxenes of the Shiant Isles Sill, Scotland. *J. Petrol.* 14, 203-230.  
LEUNG I. S., 1974: Sector-zoned titanaugites: morphology, crystal chemistry, and growth. *Am. Mineral.*, 59, 127-138.  
SMULIKOWSKI K., 1980: Uwagi o cieszyńskiej prowincji magmowej. *Rocz. Pol. Tow. Geol.*, 50, 1, 41-54.  
SEPP B., KUNZMANN T., 2001: The stability of clinopyroxene in the system CaO-MgO-SiO<sub>2</sub>-TiO<sub>2</sub> (CMST). *Am. Mineral.*, 86, 265-270.  
YAGI K., ONUMA K., 1967: The join CaMg<sub>2</sub>O<sub>6</sub>-CaTiAl<sub>2</sub>O<sub>6</sub> and its bearing on the titanaugites. *J. Fac. Sci. Hokkaido Univ. Ser. IV*, 13, 463-483.

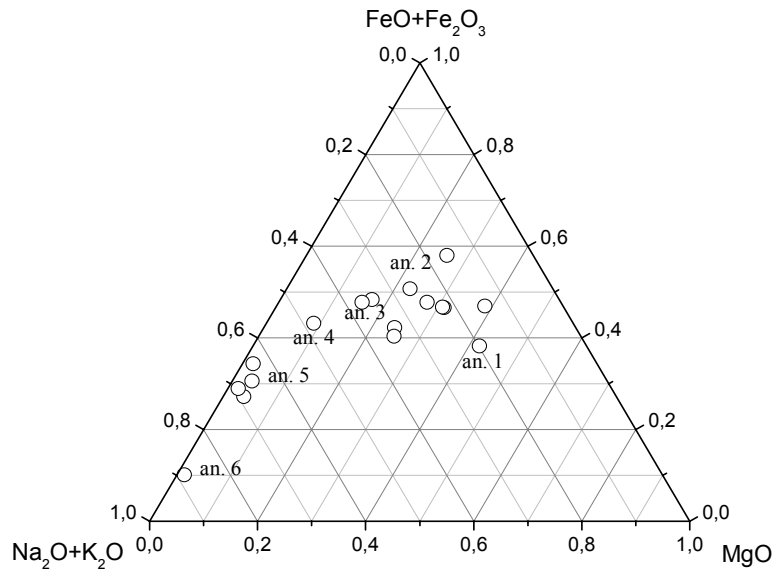
**Table 1.** Major elements of the teschenite rocks: 1 - olivine teschenite, 2 - teschenite, 3 and 4 - syenoteschenite, 5 - syenite, 6 - felsic mesostasis from syenoteschenite

	1	2	3	4	5	6
SiO <sub>2</sub>	39.74	43.44	47.20	47.61	50.41	51.96
TiO <sub>2</sub>	3.88	3.26	2.22	1.45	0.55	0.10
Al <sub>2</sub> O <sub>3</sub>	11.89	15.18	18.92	20.30	22.60	22.33
Fe <sub>2</sub> O <sub>3</sub>	2.97	4.07	3.83	2.90	1.20	0.32
FeO	7.44	7.35	5.60	4.98	2.74	1.08
MnO	0.15	0.18	0.16	0.18	0.11	0.05
MgO	11.43	5.15	3.05	1.60	0.55	0.18
CaO	12.29	12.33	7.86	6.30	6.48	4.40
Na <sub>2</sub> O	3.74	3.17	4.45	5.15	4.23	7.65
K <sub>2</sub> O	1.66	2.76	2.80	3.62	5.75	4.53
P <sub>2</sub> O <sub>5</sub>	0.54	0.67	0.69	0.29	0.16	0.55
CO <sub>2</sub>	0.97	0.83	0.00	1.03	0.00	0.70
H <sub>2</sub> O <sup>+</sup>	2.92	2.45	3.06	3.65	4.90	5.50
Total	99.62	100.84	99.84	99.06	99.68	99.35

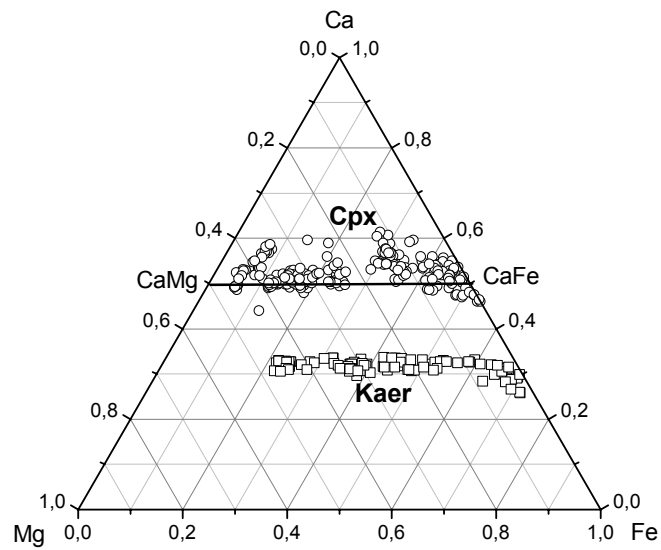
**Table 2.** Chemical analyses of pyroxene and amphibole from teschenite sill: 1 and 2 - diopside, 3 - hedenbergite, 4 - kaersutite, 5 - ferro-kaersutite, 6 – hastingsite

	1	2	3	4	5	6
SiO <sub>2</sub>	40.44	51.35	40.43	38.35	35.97	34.52
TiO <sub>2</sub>	6.05	1.10	2.28	5.58	4.22	0.59
Al <sub>2</sub> O <sub>3</sub>	11.50	1.92	9.83	14.44	12.35	13.97
Cr <sub>2</sub> O <sub>3</sub>	0.04	0.00	0.00	0.02	0.00	0.04
FeO	7.80	10.28	21.64	10.68	28.87	30.26
MnO	0.10	0.36	0.60	0.22	0.62	0.76
MgO	9.78	11.66	1.63	12.65	0.87	0.14
CaO	22.89	22.89	22.08	12.45	10.89	10.53
Na <sub>2</sub> O	0.71	0.60	0.62	2.18	2.09	1.70
K <sub>2</sub> O	0.00	0.01	0.00	1.66	2.18	2.60
Total	99.31	100.17	99.11	98.23	98.05	95.11

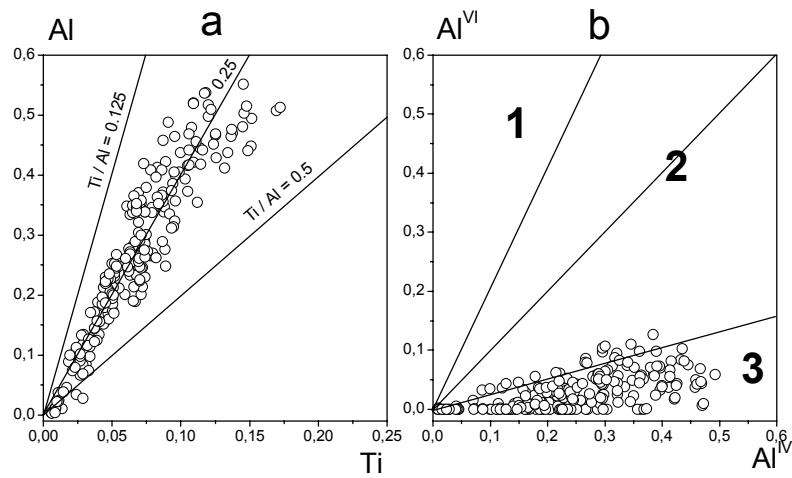
**Fig.1.** Chemical variation of teschenite rock suites. Chemical analyses of samples 1 to 6 are presented in Table 1.



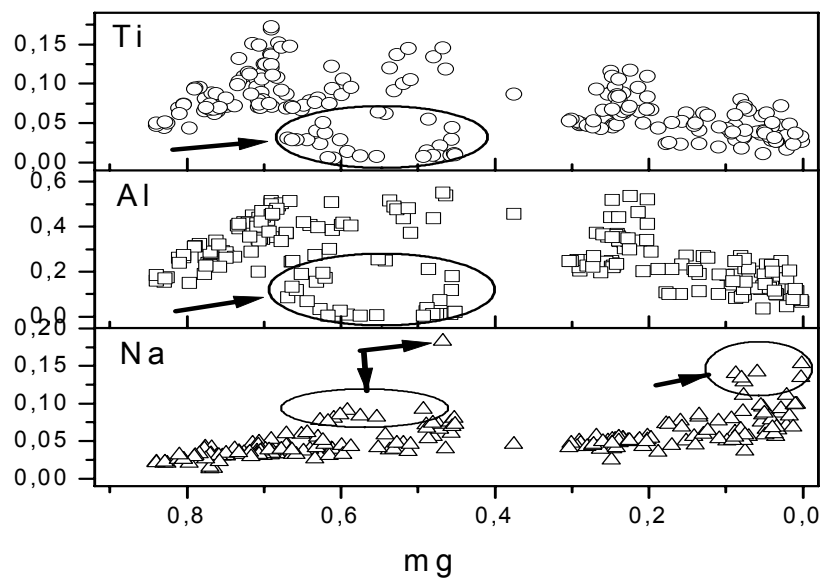
**Fig.2.** Compositions of mafic minerals plotted in Ca-Mg\_Fe (atom %; Fe=total Fe). Cpx - clinopyroxene, Kaer – kaersutite.



**Fig.3.** a - Variations of Ti and Al (cation per formula unit based on 6 O), b -  $Al^{VI}$  v.  $Al^{IV}$  in clinopyroxenes from teschenite sill. Fields: 1 - eclogites, 2 - granulites and inclusions in basalts, 3 - igneous rocks; diagram of Aoki and Shiba 1973.



**Fig.4.** Plots of Ti, Al and Na (cation per formula unit based on 6 O) v. *Mg*-number. Fig.5. Plots of Mg,  $Fe^{2+}$  and  $Fe^{3+}$  v. *mg*-number for clinopyroxenes from teschenite sill.



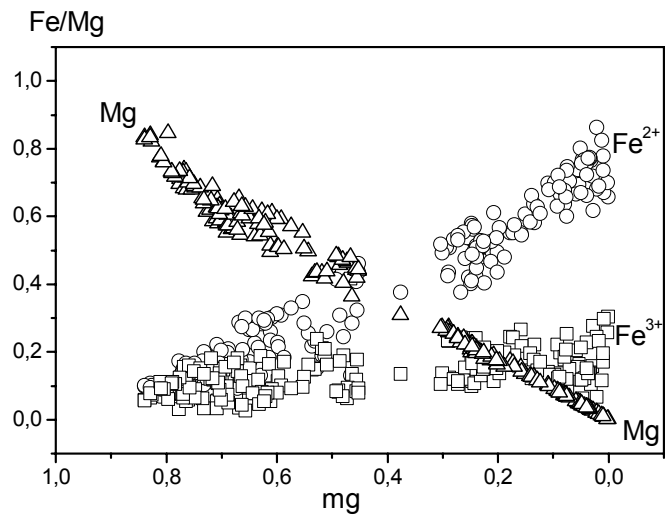


Fig. 5